A Numerical Computation of Air Flow over a Sudden Change of Surface Roughness

C. C. SHIR

IBM Research Laboratory, San Jose, Calif. 95114

(Manuscript received 21 April 1971, in revised form 6 October 1971)

ABSTRACT

This paper deals with a numerical study of the influence of changes in surface roughness on the turbulent boundary layer in the lower layer of the atmosphere under neutral conditions. The whole set of equations governing the flow is solved by a finite-difference method. The turbulent energy equation is included to provide a better understanding of turbulent mechanisms. The pressure gradient is treated implicitly. Computational results agree well with Bradley's observations. A local minimum of surface stress is found at a short distance from the edge (dividing line) in the case of smooth-to-rough transition. Two boundary layers, a velocity layer and a stress layer, are found. The height of the velocity layer is about one-half that of the stress layer. Both layers follow the 4/5 power law. The height-to-fetch ratio for the internal boundary layer is found to be about 1/10 for the stress and 1/20 for the velocity. The height-to-fetch ratio for a new nearly equilibrium layer is about 1/100 for the smooth-to-rough case and 1/200 for the rough-to-smooth case far downwind. The stress is close to the upstream value for the upper portion of the transition layer. An inflection point of the velocity profile occurs in the transition region. The non-dimensional wind shear is significantly different from the value of unity which exists in an equilibrium flow.

1. Introduction

A lower atmospheric turbulent flow above a sudden change in surface roughness has been studied extensively by several authors. Elliot (1958), Panofsky and Townsend (1964), Townsend (1965,1966), Taylor (1969, 1970), Lettau and Zabransky (1968), Blackadar *et al.* (1967), Smith (1967), Nickerson (1968), Blom and Wartena (1969), Panchov and Godev (1970), and Estoque and Bhumralkar (1969) consider this flow by using assumed forms for the velocity or shear stress profiles within an internal boundary layer developing downstream of the roughness change. Peterson (1969a) has discussed the inherent error of these approaches. Observation (Peterson, 1969b) indicates the deficiency of using a similarity method, because the non-dimensional wind shear is not equal to unity in a non-equilibrium flow. Peterson discards the similarity method, and uses the turbulent energy equation instead. Although several hypotheses are used, the method still gives more physical insight. The recent AFSOR-boundary layer conference (Kline *et al.*, 1968) indicates that the turbulent energy approach is promising. However, Peterson's result does not agree well with observation (Bradley, 1968) in the case of rough-to-smooth transition. He, like other authors, neglects the pressure gradient and the vertical equation of motion which may not be negligible in the transition layer.

In the present study, the pressure gradient and the vertical equation of motion are treated implicitly through the vorticity equation, and the horizontal stress gradient is included. The turbulent energy equation as well as equations governing the mean flow are solved by finite differences. The computational results agree well with Bradley's observations.

2. Method of analysis

The governing equations of the model are as follows:

The mean vorticity equation derived from mean horizontal and vertical momentum equations:

$$\frac{\partial\omega}{\partial t}+\mathbf{V}\cdot\nabla\omega=+\frac{\partial^2\tau}{\partial z^2}-\frac{\partial^2\tau}{\partial x^2} \tag{1}$$

The streamfunction equation derived from the continuity equation:

$$\nabla^2\psi=\omega \tag{2}$$

The turbulent energy equation:

$$\frac{\partial e}{\partial t}+\mathbf{V}\cdot\nabla e=\tau\frac{\partial U}{\partial z}-\epsilon-D. \tag{3}$$

Here ω, ψ, $\mathbf{V}$ and U are mean vorticity, streamfunction, velocity and horizontal velocity, respectively; $\tau=-\overline{u'w'}$ is the specific Reynolds stress; $e=\frac{1}{2}\overline{(u'^2+v'^2+w'^2)}$ is the mean specific turbulent energy; ϵ the dissipation rate; and D the divergence of the flux. The derivations of the governing equations are shown in the Appendix.

The following assumptions are used:

$$\tau=\alpha e, \tag{4}$$

$$\epsilon=\tau^{\frac{3}{2}}/l_\epsilon, \tag{5}$$

$$D=\frac{\partial}{\partial z}\overline{w'\left(e'+\frac{p'}{\rho_0}\right)}\approx-\frac{\partial}{\partial z}K\frac{\partial e}{\partial z}, \tag{6}$$

where $\alpha=0.22$, $K=\sqrt{\tau}l$, and

$$l_\epsilon=\begin{cases} k(z+z_0), & z\leqslant z_b,\\ \dfrac{k(z+z_0)}{1+k(z-z_b)/\lambda}, & z>z_b, \end{cases} \tag{7}$$

with $k=0.4$, $z_b=10$ m, $\lambda=40$ m.

The pressure gradient does not occur in the vorticity equation since the density variation within the transition layer is assumed to be small. The horizontal stress gradient is considered in (1), since it may not be negligible right near the edge. The value of α is obtained from Cramer's (1967) Round Hill data. Peterson (1969a) uses $\alpha=0.16$ according to Cramer's data based on an hourly average value. Cramer believes the value of 0.22 is appropriate (private communication). Harsha and Lee (1970) obtained the value of 0.3 after they examined 500 sets of data. Bradshaw *et al.* (1967) used the value of 0.3 which was mistaken as 0.15 by Peterson (1969a). Bradshaw and Ferriss (1963) believe α is a slowly varying function of the ratio of production to dissipation of the turbulent energy and is about 0.3 in laboratory turbulent boundary layers. However, the value of α could be smaller in the atmosphere. But there is not sufficient data to enable us to fully understand the behavior of α. The length l_ϵ, which (according to Bradshaw and Ferriss) may be a universal function, must be determined empirically. Bradshaw found that l_ϵ is equal to kz near the wall and tends to a constant value away from the wall. Insufficient data are available to derive the form of l_ϵ for atmospheric turbulent flow. In Eq. (7), l_ϵ is assumed to be linear near the surface and to tend gradually to the constant value of λ. It is a modified form of Blackadar's (1962) formula.

The energy flux D is assumed to be of the gradient diffusion type. Another form of hyperbolic type for large eddies is used by Bradshaw. The hyperbolic type may be significant under unstable conditions, just as the gradient type is under stable conditions. In neutral flow, both approaches may be equally realistic. The form of K is assumed equal to $\sqrt{\tau}l$ with $l=l_\epsilon$. A different form, $K=\tau/(\partial U/\partial z)$, is used by Peterson (1969a), although this form is more difficult to program due to possible small value of $\partial U/\partial z$. Both forms have been studied. However, in the present study neither form of K affects the results a great deal.

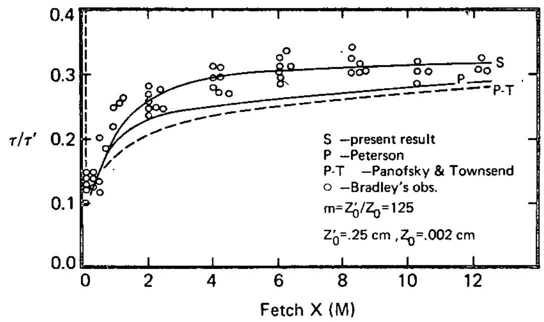

FIG. 2. Comparison of surface stress variation with fetch for the model and for various observations ($z_0'=0.25$ cm, $z_0=0.002$ cm).

The boundary conditions are

$\tau=\tau'$, $U=U'$, for $x\leqslant 0$ (upstream boundary)

$\sqrt{\tau}=kz_0\partial U/\partial z|_0$, $U=0$, $W=0$, for $z=0$ (lower boundary)

$\tau=\tau'$, $U=U'$, for $z=h$ (upper boundary)

where the prime denotes the upstream value. The details of the finite-difference scheme are discussed by Shir (1970); the configuration of the model is shown in Fig. 1.

3. Computational results

The computational results are compared here with observations and other theories.

a. Surface Reynolds stress

1) ROUGH-TO-SMOOTH TRANSITION

The normalized surface stress reacts abruptly to a sudden roughness change, it overshoots, and then

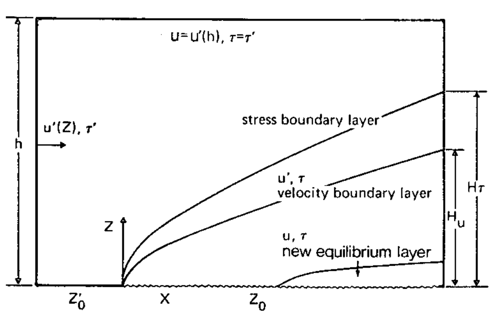

FIG. 1. The configuration of the model.

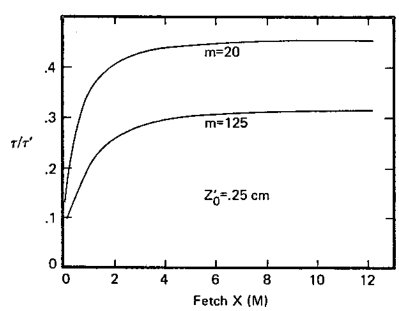

FIG. 3. Variation of surface stress with fetch for different roughness ratios ($z_0'=0.25$ cm, $m=z_0'/z_0=20$, 125).

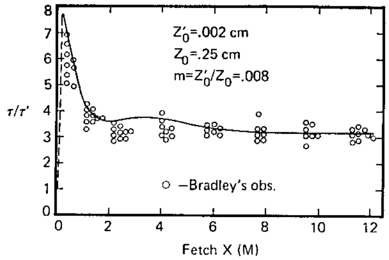

FIG. 4. Same as Fig. 2 except for $z_0'=0.002$ cm, $z_0=0.25$ cm.

slowly approaches a constant value of 0.32. In Fig. 2, with roughness changing from 0.25 to 0.002 cm, the present result agrees well with Bradley's data, while other theories (Peterson, 1969a; Panofsky and Townsend, 1964) predict lower values. The low value of Peterson's result could be due to neglecting the pressure gradient and the vertical equation of motion. Panofsky and Townsend's method predicts an even lower value than Peterson's. In Fig. 3 the increase of downwind roughness to $z_0=0.0125$ cm raises the final constant value to 0.425.

2) SMOOTH-TO-ROUGH TRANSITION

With a roughness change from 0.002 to 0.25 cm, the stress overshoots and then gradually approaches a constant value of 3.10 (Fig. 4). This agrees well with observation. However, a local minimum is found near 2 m from the edge (dividing line). The stress has two oscillations before it reaches the final value. Bradley (1968) also noticed this phenomena of a local minimum near 2 m in his observation, although he did not draw any conclusion since it had not been predicted by theory. It is not clear why the local minimum occurs only in decelerated flow (smooth-to-rough transition), but not in accelerated flow (rough-to-smooth transition). In Fig. 5 the surface stress ratio (downstream stress to upstream stress) decreases with larger roughness ratio. A local minimum also occurs at a shorter distance from the edge for larger roughness ratio.

b. Boundary layer height

The height of the internal boundary layer is important for the choice of a testing site. Unfortunately, the definition of the internal boundary layer is inconsistent among various authors. Some define the boundary according to the velocity profile, while others use the stress profile. In the present study, two boundary layers are defined, viz., velocity boundary layer and stress boundary layer. The height of the velocity layer (H_u) is determined where the downstream velocity is within 1% of the upstream velocity. An analogous definition is used for the height of the stress layer (H_τ). In Fig. 6 the height of the velocity layer agrees well with Bradley's observation in which he determines the height by the velocity profile. The height of the velocity layer for rough-to-smooth transition and for smooth-to-rough transition follows a 4/5 power law closely. The slope of the boundary is larger for smooth-to-rough transition ($m=1/125$, $z_0=0.25$ cm). In Fig. 7 the heights of the velocity layer, with different downstream roughnesses and different roughness ratios, are shown. For smooth-to-rough transition with the same downstream roughness, the height of the boundary increases with larger roughness ratio, but the slope of the boundary remains the same. A similar result is found for rough-to-smooth transition with the same upstream roughness. This suggests the following re-

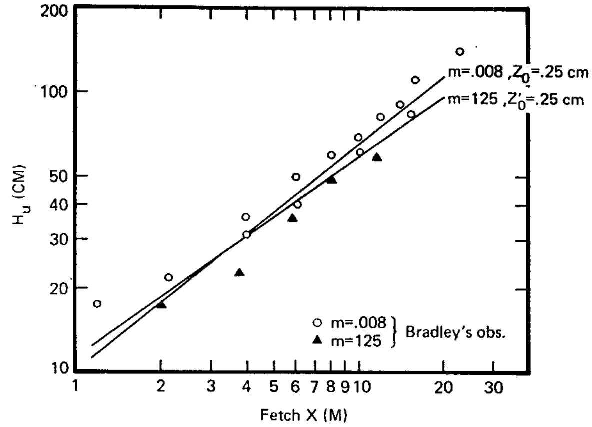

FIG. 6. Comparison of the height of the model velocity boundary layer (H_u) with observations for different roughnesses ($z_0'=0.25$ cm, $m=125$ and $z_0=0.25$ cm, $m=0.008$).

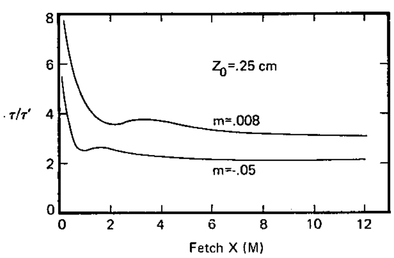

FIG. 5. Same as Fig. 3 except for $z_0=0.25$ cm. $m=0.05$, 0.008.

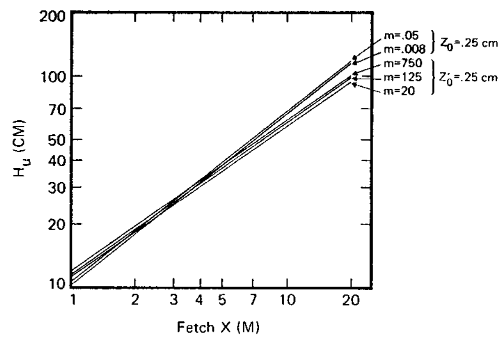

FIG. 7. Variation of the height of the velocity boundary layer (H_u) with fetch for different roughness ratios ($z_0'=0.25$ cm, $m=750$, 125, 20; $z_0=0.25$ cm, $m=0.05$, 0.008).

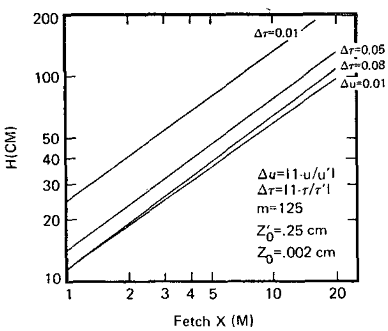

FIG. 8. Variation of the height of the stress and velocity boundary layers with fetch ($z_0'=0.25$ cm, $z_0=0.002$ cm).

lation for the height of the velocity layer:

$$H_u \approx f_1\left(\frac{z_0'}{z_0}\right) X^{0.8+f_2(z_0'/z_0)}. \quad (8)$$

In Fig. 8 computed heights of the stress and velocity layer are shown. The height of stress layer is about 2.2 times the height of the velocity layer. That is, the velocity adjusts itself to the new roughness more slowly than the stress. At the boundary of the velocity layer, the stress is about within 8% of the upstream value. In Fig. 9, the case of smooth-to-rough transition, the height of the stress layer is about twice the height of velocity layer. The height-to-fetch ratio is about 1/10 for the stress layer and 1/20 for the velocity layer.

c. Wind Profile

In Fig. 10, the case of smooth-to-rough transition, the normalized wind profile (normalized to the wind at 2.2 m) at several downwind distances are compared with Bradley's observation. Agreement is good at far downwind (curves A and B) above the rough surface ($z_0=0.25$ cm). The discontinuity in the velocity gradient is quite sharp. An inflection point of the velocity profile does occur as pointed out by Peterson (1969a). The inflection point makes the velocity profile at higher altitudes close to the upstream velocity. As a consequence, the velocity layer is much lower than the stress layer. Near the smooth surface ($z_0'=0.002$ cm), the computed velocity is smaller than that shown by Bradley's data above 20 cm. One possible explanation is that the wind speed at 2.2 m above the transition region is held constant downwind in this study. However, Bradley's data show that the wind speed at 2.2 m increases 38% downwind from the edge and then decreases. As a consequence, the normalized wind speed is larger near the edge where the wind speed at 2.2 m is smaller. This leads to an inconsistancy in his data. Curve E, which (according to Bradley) corresponds to roughness $z_0'=0.002$ cm, actually has a larger slope than the velocity profile with that roughness (curve D). He also questioned the accuracy of the estimated roughness. However, it is not clear how the wind speed above the transition region can have such a large variation (as high as 80%). Similarly, in Fig. 11, the case of rough-to-smooth transition, the computed wind profiles agree well with observation near the rough surface but are smaller far downwind above the smooth surface ($z_0=0.002$ cm). The wind profile changes sharply and has an inflection point.

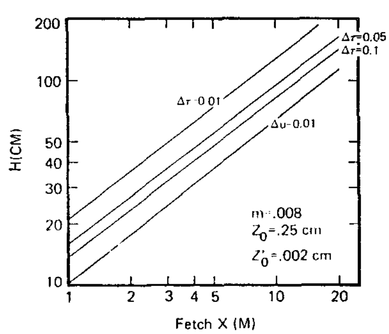

FIG. 9. Same as Fig. 8 except for $z_0'=0.022$ cm, $z_0=0.25$ cm.

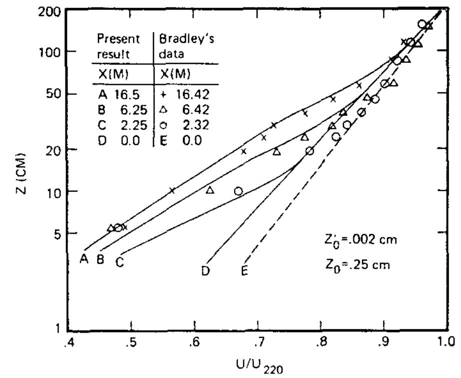

FIG. 10. Comparison of model and observed wind profiles for $z_0'=0.002$ cm, $z_0=0.25$ cm.

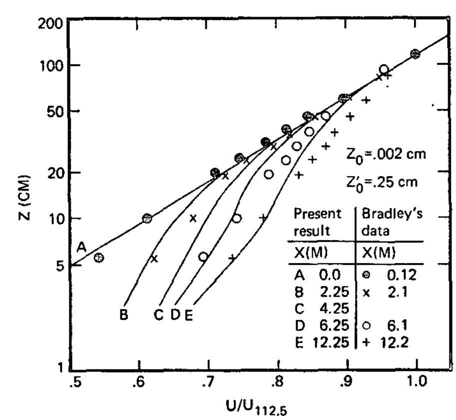

FIG. 11. Same as Fig. 10 except for $z_0'=0.25$ cm, $z_0=0.002$ cm.

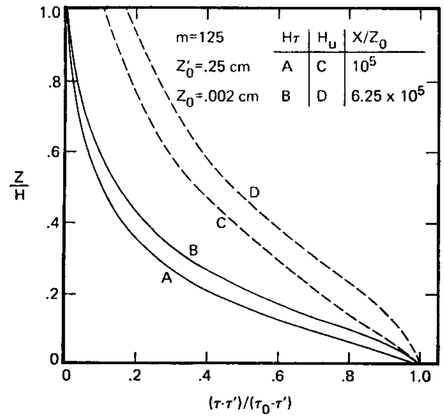

FIG. 12. Normalized stress distribution within the stress and velocity boundary layers ($z_0'=0.25$ cm, $z_0=0.002$ cm).

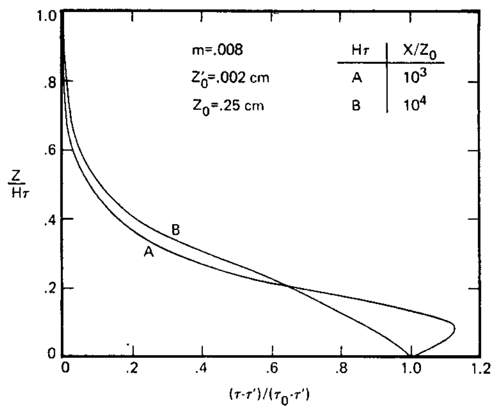

FIG. 13. Normalized stress distribution within the stress boundary layer ($z_0'=0.002$ cm, $z_0=0.25$ cm).

d. Vertical distribution of stress

Although observations on the stress above the surface are not available, a computed stress distribution is shown in Fig. 12. If we use the height of the stress layer (H_τ), the stress inside the transition region is closer to the upstream stress (τ') than the surface stress (τ_0) for the upper 75% of the layer, as pointed out by Peterson. However, according to the velocity layer (H_u), only the stress for the upper 50% of the layer is close to the upstream value. Hence, the definition of the internal boundary layer is rather important. Discrepancy between different theories may arise from using different definitions. Moreover, the stress distribution is neither linear nor self-similar at various downwind distances. In Fig. 13, the case of smooth-to-rough transition, the stress decreases with height and then increases near the edge (curve A). The stress for the upper 75% of the layer is close to the upwind stress. This suggests that the K theory widely used in urban heat island simulation, in which the stress is assumed to adjust itself to the new surface immediately, is not a good approximation, because the stress above the new surface is still dominated by the upwind stress. In Fig. 14 the contours of constant stress show growth slightly less than linear with increasing downwind fetch. Near

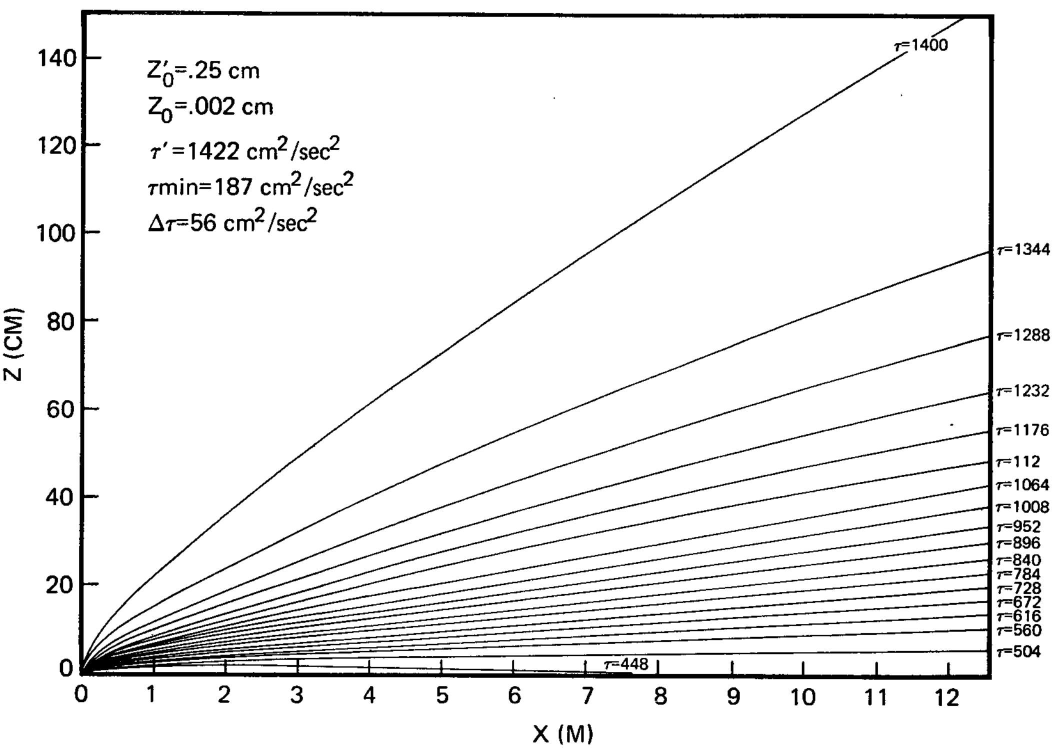

FIG. 14. Stress distribution ($z_0'=0.25$ cm, $z_0=0.002$ cm, plotting stress interval $\Delta\tau=56$ cm^2 sec^{-2}).

the edge, the horizontal stress gradient, which is neglected by other theories, is not small.

e. Non-dimensional wind shear

In Fig. 15 we show the important parameter, the non-dimensional wind shear. In the case of rough-to-smooth transition (curves A and B) the non-dimensional wind shear decreases 50% from unity, and increases about 50% in the case of smooth-to-rough transition. This is also pointed out by Peterson (1969b) from theoretical considerations and observations. The assumption that the non-dimensional wind shear is equal to unity is not a good approximation inside the transition region.

Moreover, the non-dimensional wind shear far downwind is about unity (within 10%) for the lowest tenth of the transition layer in the smooth-to-rough case, and for only the lowest twentieth of that layer in the rough-to-smooth case. Consistent with this, the shear stresses for the smooth-to-rough case (Fig. 13) are within 10% of the surface values throughout the lowest tenth of the transition layer far downwind. On the other hand, the shear stresses for the rough-to-smooth case (Fig. 12) are within 10% of the surface values only in the lowest twentieth of the transition layer. The velocity profiles in Figs. 10 and 11 are close to logarithmic for the lowest 10% of the transition layer. These indicate that the flow is close to a new equilibrium in the lowest portion of the transition layer far downwind. The height-to-fetch ratio for a nearly equilibrium layer is about 1/100 for the smooth-to-rough case and 1/200 for the rough-to-smooth case far downwind. Near the edge, the flow does not seem close to equilibrium.

4. Discussion and summary

The theory developed here leads to fairly good agreement with observation: the surface Reynolds stress changes rapidly near the edge; a local minimum occurs at a short distances from the edge in the case of smooth-to-rough transition; and the height of the boundary layer closely follows the 4/5 power law. However, the slope of the boundary depends on the type of transition. In the transition region, the velocity reacts to the new surface more slowly than the stress. Hence, the height of the stress layer is about twice that of the velocity layer. The controversial height-to-fetch ratio is found to be about 1/10 for the stress and 1/20 for the velocity. Then the height-to-fetch ratio for the new equilibrium layer may be about 1/100 for the smooth-to-rough case and 1/200 for the rough-to-smooth case far downwind.

Although the theory seems to be adequate for this simple case, more observations are needed for the evaluation and extension of the model to more complicated cases. The stress-to-turbulent-energy ratio, especially, which is well studied for laboratory flow, is nowhere near as well understood for atmospheric flow,

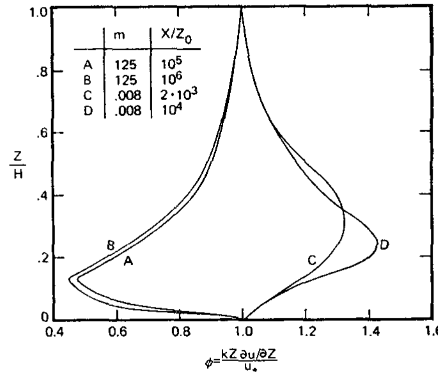

FIG. 15. Non-dimensional wind shear distribution within stress boundary layer ($z_0'=0.25$ cm, $z_0=0.002$ cm and $z_0'=0.002$ cm, $z_0=0.25$ cm).

and the length (l_ϵ), which may be a universal function, needs further investigation.

Acknowledgements. The author is grateful to Mr. J. E. Fromm and Dr. J. A. Barker for proofreading the manuscript.

APPENDIX

Derivation of the Model Equations

In the lowest atmospheric layer, the mean momentum equations with the Boussinesq approximation (Panofsky and Lumley, 1964; Spiegel and Veronis, 1960) are

$$\frac{\partial \mathbf{V}}{\partial t}+\mathbf{V}\cdot\nabla\mathbf{V}=-\nabla\cdot\overline{\mathbf{v}'\mathbf{v}'}-\frac{1}{\rho_m}\nabla P'-\frac{T'}{T_m}\mathbf{g}+\nu\nabla^2\mathbf{V},\quad \text{(A1)}$$

where $\mathbf{V}=(U,0,W)$ is the mean velocity, P' and T' are the mean pressure and temperature deviation from the hydrostatic state, ρ_m and T_m the average density and temperature over the whole layer, ν the kinematic viscosity, and $\mathbf{v}'=(u',v',w')$ the fluctuation velocity.

The mean vorticity equation derived from (A1) under neutral conditions is

$$\frac{\partial \omega}{\partial t}+\mathbf{V}\cdot\nabla\omega=-\frac{\partial^2\overline{u'w'}}{\partial z^2}+\frac{\partial^2\overline{u'w'}}{\partial x^2}-\frac{\partial^2}{\partial x\partial z}(\overline{u'^2}-\overline{w'^2})+\nu\nabla^2\omega,\quad \text{(A2)}$$

where the viscous term can be neglected in comparison with turbulence stress terms. The third term on the right is often small except right near the edge. The present model cannot compute this term unless certain assumptions are supplied. Eq. (A2) is thus approximated by

$$\frac{\partial \omega}{\partial t}+\mathbf{V}\cdot\nabla\omega=\frac{\partial^2\tau}{\partial z^2}-\frac{\partial^2\tau}{\partial x^2},\quad \text{(A3)}$$

where $\tau=-\overline{u'w'}$ is the specific Reynolds stress.

The turbulent energy equation for the neutral conditions is

$$\frac{\partial e}{\partial t}+\mathbf{V}\cdot\nabla e=\tau\frac{\partial U}{\partial z}-(\overline{u'^2}-\overline{w'^2})\frac{\partial U}{\partial x}+\tau\frac{\partial W}{\partial x}-\epsilon-D. \quad \text{(A4)}$$

In (A4) the third term on the right can be neglected in comparison with the first term. The second term may not be negligible near the edge. However, this term cannot be computed with the present model.

Eq. (A4) thus simplifies to

$$\frac{\partial e}{\partial t}+\mathbf{V}\cdot\nabla e=\tau\frac{\partial U}{\partial z}-\epsilon-D. \quad \text{(A5)}$$

REFERENCES

Blackadar, A. K., 1962: The vertical distribution of wind and turbulent exchange in a neutral atmosphere. *J. Geophys. Res.*, **67**, 3095–3102.

——, P. E. Glass and H. A. Panofsky, 1967: Effect of stability on the wind profile under conditions of inhomogeneous terrain roughness, *Proc. U. S. Atomic Energy Commission Conf.* Chalk River, Ontario, 453–461.

Blom, J., and L. Wartena, 1969: The influence of changes in surface roughness on the development of the turbulent boundary layer in the lowest layer of the atmosphere. *J. Atmos. Sci.*, **26**, 255–265.

Bradley, E. F., 1968: A micrometeorological study of velocity profiles and surface drag in the region modified by a change in surface roughness. *Quart. J. Roy. Meteor. Soc.*, **94**, 361–379.

Bradshaw, P., and D. H. Ferriss, 1963: Derivation of a shear-stress transport equation from the turbulent energy equation. *Proc. Conf. Computation of Turbulent Boundary Layers*, Stanford University, Calif., 264–274.

——, ——, and N. P. Atwell, 1967: Calculation of boundary-layer development using the turbulent energy equation. *J. Fluid. Mech.*, **28**, 593–616.

Cramer, H. E., 1967: Turbulent transfer processes for quasi-homogeneous flow within the atmospheric surface layer. *Phys. Fluids*, **10**, No. 9, Pt. II, 240–246.

Elliott, W. P., 1958: The growth of the atmospheric internal boundary layer. *Trans. Amer. Geophys. Union*, **39**, 1048–1054.

Estoque, M. A., and C. M. Bhumralkar, 1969: Further studies on flow over nonhomogeneous terrain. Tech. Rept., Div. of Atmospheric Science, University of Miami.

Harsha, P. T., and S. C. Lee, 1970: Correlation between turbulent shear stress and turbulent kinetic energy. *AIAA. J*, **8**, 1508–1510.

Kline, S. J., *et al.*, 1968: *Proc. Conf. Computation of Turbulent Boundary Layers.* Stanford University, Calif.

Lettau, H., and J. Zanbransky, 1968: Interrelated changes of wind profile structure, and Richardson number in air flow from land to inland lakes. *J. Atmos. Sci.*, **25**, 718–728.

Nickerson, E. C., 1968: Boundary layer adjustment as an initial value problem. *J. Atmos. Sci.*, **25**, 207–213.

Panchov, S., and N. Godev, 1970: Wind profile and vertical motions above an abrupt change in surface roughness and temperature. *Proc. Symp. Planetary Boundary Layer*, Boulder, Colo.

Panofsky, H., and J. Lumley, 1964: *The Structure of Atmosphere Turbulence.* New York, Interscience, 239 pp.

——, and A. A. Townsend, 1964: Changes of terrain roughness and wind profile. *Quart. J. Roy. Meteor. Soc.*, **90**, 147–155.

Peterson, E. W., 1969a: Modification of mean flow and turbulent energy by a change in surface roughness under conditions of neutral stability. *Quart. J. Roy. Meteor. Soc.*, **95**, 561–575.

——, 1969b: On the relation between the shear stress and the velocity profile after a change in surface roughness. *J. Atmos. Sci.*, **26**, 773–774.

Shir, C. C., 1970: A pilot study in numerical techniques for predicting air pollutant distribution downwind from a line stack. *Atmos. Environ.*, **4**, 387–407.

Smith, F. B., 1967: Modification of wind profile due to changes in surface roughness. *Proc. U. S. Atomic Energy Commission Conf.* Chalk River, Ontario, 463–475.

Spiegel, E., and G. Veronis, 1960: On the Boussinesq approximation for a compressible fluid, *Astrophy. J.*, **131**, 442–447.

Taylor, P. A., 1969: The planetary boundary layer above a change in surface roughness. *J. Atmos. Sci.*, **26**, 432–440.

——, 1970: A model of airflow changes in surface heat flux, temperature and roughness for neutral and unstable conditions. *Boundary Layer Meteor.*, **1**, 18–39.

Townsend, A. A., 1965: The response of a turbulent boundary layer to abrupt changes in surface conditions. *J. Fluid Mech.*, **22**, 799–882.

——, 1966: The flow in a turbulent boundary layer after a change in surface roughness. *J. Fluid Mech.*, **26**, 255–266.